

1
2 High Frequencies of Phenotypically and Functionally Senescent and Exhausted CD56⁺CD57⁺PD-1⁺
3 Natural Killer Cells, SARS-CoV-2-Specific Memory CD4⁺ and CD8⁺ T cells Associated with Severe
4 Disease in Unvaccinated COVID-19 Patients

5
6 Ruchi Srivastava¹; Nisha Dhanushkodi¹; Swayam Prakash¹; Pierre Gregoire Coulon¹;
7 Hawa Vahed^{1, 3}; Latifa Zayou¹, Afshana Quadiri¹, and Lbachir BenMohamed^{1, 2, 3, 4*}

8
9 ¹Laboratory of Cellular and Molecular Immunology, Gavin Herbert Eye Institute, University of
10 California Irvine, School of Medicine, Irvine, CA 92697; ²Department of Molecular Biology &
11 Biochemistry; and ³Department of Vaccines and Immunotherapies, TechImmune, LLC, University Lab
12 Partners, Irvine, CA 92660-7913; ⁴Institute for Immunology; University of California Irvine, School of
13 Medicine, Irvine, CA 92697.

14
15 Running Title: Senescent and Exhausted NK and T cells in Critically ill COVID-19 Patients

16
17
18 Keywords: SARS-CoV-2, COVID-19, senescence, NK cells, CD8⁺ T cells

19
20 *Corresponding author: Dr. Lbachir BenMohamed, Laboratory of Cellular and Molecular Immunology,
21 Gavin Herbert Institute; Hewitt Hall, Room 232; 843 Health Sciences Rd; Irvine, CA 92697-4390;
22 Phone: 949-824-8937; Fax: 949-824-9626; E-mail: Lbenmoha@uci.edu

23
24 Conflict of interest: The authors have declared that no conflict of interest exists

25
26 §Footnotes: This work is supported by Public Health Service Research R01 Grants EY026103,
27 EY019896, and EY024618 from the National Eye Institute (NEI) and R21 Grant AI110902 from the
28 National Institutes of Allergy and Infectious Diseases (NIAID) (to L.BM.), and in part by The Discovery
29 Center for Eye Research (DCER) and the Research to Prevent Blindness (RPB) grant

30

31

32

ABSTRACT

33

34

35

36

37

38

39

40

41

42

43

44

45

46

47

48

49

50

51

52

Unvaccinated COVID-19 patients display a large spectrum of symptoms, ranging from asymptomatic to severe symptoms, the latter even causing death. Distinct Natural killer (NK) and CD4⁺ and CD8⁺ T cells immune responses are generated in COVID-19 patients. However, the phenotype and functional characteristics of NK cells and T-cells associated with COVID-19 pathogenesis versus protection remain to be elucidated. In this study, we compared the phenotype and function of NK cells SARS-CoV-2-specific CD4⁺ and CD8⁺ T cells in unvaccinated symptomatic (SYMP) and unvaccinated asymptomatic (ASYMP) COVID-19 patients. The expression of senescent CD57 marker, CD45RA/CCR7 differentiation status, exhaustion PD-1 marker, activation of HLA-DR, and CD38 markers were assessed on NK and T cells from SARS-CoV-2 positive SYMP patients, ASYMP patients, and Healthy Donors (HD) using multicolor flow cytometry. We detected significant increases in the expression levels of both exhaustion and senescence markers on NK and T cells from SYMP patients compared to ASYMP patients and HD controls. In SYMP COVID-19 patients, the T cell compartment displays several alterations involving naive, central memory, effector memory, and terminally differentiated T cells. The senescence CD57 marker was highly expressed on CD8⁺ T_{EM} cells and CD8⁺ T_{EMRA} cells. Moreover, we detected significant increases in the levels of pro-inflammatory TNF- α , IFN- γ , IL-6, IL-8, and IL-17 cytokines from SYMP COVID-19 patients, compared to ASYMP COVID-19 patients and HD controls. The findings suggest exhaustion and senescence in both NK and T cell compartment is associated with severe disease in critically ill COVID-19 patients.

53 **IMPORTANCE**

54

55 Unvaccinated COVID-19 patients display a large spectrum of symptoms, ranging from
56 asymptomatic to severe symptoms, the latter even causing death. Distinct Natural killer (NK) and
57 CD4⁺ and CD8⁺ T cells immune responses are generated in COVID-19 patients. In this study, we
58 detected significant increases in the expression levels of both exhaustion and senescence markers on
59 NK and T cells from unvaccinated symptomatic (SYMP) compared to unvaccinated asymptomatic
60 (ASYMP) COVID-19 patients. Moreover, we detected significant increases in the levels of pro-
61 inflammatory TNF- α , IFN- γ , IL-6, IL-8, and IL-17 cytokines from SYMP COVID-19 patients, compared
62 to ASYMP COVID-19 patients. The findings suggest exhaustion and senescence in both NK and T
63 cell compartment is associated with severe disease in critically ill COVID-19 patients.

64

65

TWEET

66

67 Significant exhaustion and senescence in both NK and T cells were detected in unvaccinated
68 symptomatic COVID-19 patients, suggesting a weakness in both innate and adaptive immune
69 systems leads to severe disease in critically ill COVID-19 patients.

70

INTRODUCTION

Severe acute respiratory syndrome coronavirus 2 (SARS-CoV-2) is a β -Coronavirus that was first detected in 2019 in Wuhan, China. In the ensuing months, it has been transmitted worldwide. As of July 2022, more than 568 million people have contracted coronavirus disease (COVID-19), the pandemic that has killed approximately 6.38 million people globally (1). COVID-19, caused by SARS CoV-2, has a wide range of clinical manifestations, ranging from asymptomatic to severe symptomatic disease (2). Therefore, understanding the clinical and immunological characteristics of unvaccinated ASYMP and SYMP COVID-19 patients holds significance in elucidating the immunopathogenesis of COVID-19 and informing the development of effective immune treatments. Within 2-14 days after SARS-CoV-2 exposure, newly infected individuals may develop fever, fatigue, myalgia, and respiratory symptoms, including cough and shortness of breath (3, 4). While the majority (80-85%) of newly infected individuals are asymptomatic (i.e., patients who remain symptomless despite being SARS-CoV-2-positive), a minority of individuals are symptomatic, especially the elderly and those with compromised health, that develop severe pulmonary inflammatory disease and may need a rapid medical intervention to prevent acute respiratory distress syndrome and death (5-10).

Innate and adaptive immune responses are of great significance for the control of viral infections. NK cells exert the primary control during acute viral infection, but CD4⁺ and cytotoxic CD8⁺ T lymphocytes (CTLs) are critical for the long-term surveillance (11). Recently, De Biasi et al. reported an increase in the CD57 expression on CD8⁺ T cells (12, 13). CD57 is a key marker of *in vitro* replicative senescence and is associated with prolonged chronic infection (14). Immunosenescence includes a shift towards less functional T cells in the immune system (15). However, CD57 expression is reported to be a marker of mature NK cells. The phenotypes and differentiation status associated with replicative senescent T lymphocytes are not well-defined. Like T-cells, NK cell expression of CD57 could be considered as a marker of terminal differentiation (16).

96 Furthermore, the expression of CD57 aids in identifying the final stages of peripheral NK cell
97 maturation, and the expression of CD57 increases with age and chronic infections (16).

98 Reports show that repeated T cell activation is associated with terminally differentiated cells
99 and the corresponding upregulation of CD57 (13, 17). It is observed that shortened telomeres are
100 features of senescent cells, and replicative senescence results in a low proliferative capacity of the
101 cells, eventually leading to an inability to eradicate infection (18).

102 Understanding the spectrum of innate and adaptive immune responses against SARS-CoV2,
103 disease severity, and cellular immunosenescence in SARS-CoV-2 infected symptomatic versus
104 asymptomatic individuals can ultimately inform the identification of new therapeutic targets. To attain
105 this goal, we phenotypically and functionally characterized the senescence markers (CD57),
106 differentiation status (CD45RA/CCR7), exhaustion marker (PD-1), and activation marker (HLA-DR
107 and CD38) from patients with SARS-CoV-2 positive symptomatic and asymptomatic patients, and
108 Healthy controls using multicolor flow cytometry.

109 In this report, we show 1) a decreased CD56^{bright} NK cell population and higher frequency of
110 mature/terminally differentiated NK cells (CD57⁺) in SYMP patients; 2) the activation status,
111 senescence, and exhaustion profile were significantly increased in COVID-19 SYMP individuals; 3)
112 SARS-CoV-2 specific senescent T cells with an effector memory phenotype (CD57⁺CD8⁺ T_{EM} and
113 CD57⁺CD8⁺ T_{EMRA} cells) was detected in COVID-19 SYMP individuals; 4) COVID-19 patients
114 displayed increased cytokine storm detectable in the plasma samples.

115 Our findings demonstrate that increased T cell exhaustion and senescence markers in
116 unvaccinated ASYMP COVID-19 patients compared to unvaccinated ASYMP COVID-19 patients and
117 Healthy Controls. Furthermore, T cell senescence markers were highly expressed on CD8⁺ T_{EM} and
118 CD8⁺ T_{EMRA} cells than on T_{Naive} and T_{CM} cells. These results suggest that the upregulation of
119 exhaustion and senescence pathways during symptomatic COVID-19 may affect both NK and T cell
120 compartments, leading to inefficient clearance of SARS-CoV-2 infection and severe disease.

121

MATERIALS & METHODS

Human study population: All clinical investigations in this study were conducted according to the Declaration of Helsinki principles. All subjects were enrolled at the University of California, Irvine, under approved Institutional Review Board-approved protocols (IRB#-2020-5779). Written informed consent was received from all participants before inclusion. Twenty COVID-19 patients (Asymptomatic and Symptomatic) and ten unexposed Healthy individuals, who had never been exposed to SARS-CoV-2 or COVID-19 patients, were enrolled in this study (**Table 1**). Thirty percent were Caucasian, and 70% were non-Caucasian. Forty-four percent were females, and 60% were males with an age range of 21-67 years old (median 39). None of the symptomatic patients were on anti-viral or anti-inflammatory drug treatments during blood sample collections.

Detailed clinical and demographic characteristics of the symptomatic versus asymptomatic COVID-19 patients and the unexposed Healthy individuals concerning age, gender, HLA-A*02:01, and HLA-DR distribution, COVID-19 disease severity, comorbidity, and biochemical parameters are detailed in **Table 1**.

HLA-A2 typing: The HLA-A2 status was confirmed by PBMCs staining with 2 μ L of anti-HLA-A2 mAb (clone BB7.2) (BD Pharmingen, Franklin Lakes, NJ), at 4°C for 30 minutes. The cells were washed and analyzed by flow cytometry using an LSRII (Becton Dickinson, Franklin Lakes, NJ). The acquired data were analyzed with FlowJo software (BD Biosciences, San Jose, CA).

Tetramer/ peptide staining: Fresh PBMCs were analyzed for the frequency of CD8⁺ T cells recognizing the SARS-CoV-2 peptide/tetramer complexes, as we previously described in (19). The cells were incubated with SARS-CoV-2 peptide/tetramer complex for 30–45 min at 37°C. The cell preparations were then washed with FACS buffer and stained with FITC-conjugated anti-human CD8 mAb (BD Pharmingen). Finally, the cells were washed and fixed with 1% paraformaldehyde in PBS

148 and subsequently acquired on a BD LSRII. Data were analyzed using FlowJo version 9.5.6 (Tree
149 Star).

150

151 ***Human peripheral blood mononuclear cells (PBMC) isolation:*** SARS-COV-2 positive
152 individuals were recruited at the UC Irvine Medical Center. Between 40 -50 mL of blood was drawn
153 into yellow-top Vacutainer[®] Tubes (Becton Dickinson). The plasma samples were isolated and stored
154 at -80°C for the detection of various cytokines using Luminex. PBMCs were isolated by gradient
155 centrifugation using a leukocyte separation medium (Life Sciences, Tewksbury, MA). The cells were
156 then washed in PBS, and re-suspended in a complete culture medium consisting of RPMI1640, 10%
157 FBS (Bio-Products, Woodland, CA) supplemented with 1x penicillin/streptomycin/L-glutamine, 1x
158 sodium pyruvate, 1x non-essential amino acids, and 50 µM of 2-mercaptoethanol (Life Technologies,
159 Rockville, MD). For future testing, freshly isolated PBMCs were also cryopreserved in 90% FCS and
160 10% DMSO in liquid nitrogen.

161

162 ***Human T cells flow cytometry assays:*** The following anti-human antibodies were used for
163 the flow cytometry assays: CD3 Percp, CD8 APC-Cy7, CD57 PE-Cy7, PD-1 A647, CD45RA FITC,
164 CCR7 BV786, HLA-DR BUV385, CD38 A700, CD56 APC (BioLegend, San Diego, CA). For surface
165 staining, mAbs against cell markers were added to a total of 1×10^6 cells in 1X PBS containing 1%
166 FBS and 0.1% sodium azide (FACS buffer) for 45 minutes at 4°C. After washing with FACS buffer,
167 cells were permeabilized for 20 minutes on ice using the Cytofix/Cytoperm Kit (BD Biosciences) and
168 then washed twice with Perm/Wash Buffer (BD Biosciences). Intracellular cytokine mAbs were then
169 added to the cells and incubated for 45 minutes on ice in the dark. Finally, cells were washed with
170 Perm/Wash and FACS Buffer and fixed in PBS containing 2% paraformaldehyde (Sigma-Aldrich, St.
171 Louis, MO). For each sample, 100,000 total events were acquired on the BD LSRII. Ab capture beads
172 (BD Biosciences) were used as individual compensation tubes for each fluorophore in the

173 experiment. We used fluorescence minus controls for each fluorophore to define positive and
174 negative populations when initially developing staining protocols. In addition, we further optimized
175 gating by examining known negative cell populations for background expression levels. The gating
176 strategy was similar to that used in our previous work (20). Briefly, we gated on single cells, dump
177 cells, viable cells (Aqua Blue), lymphocytes, CD3⁺ cells, and human epitope-specific CD8⁺ T cells
178 using HSV-specific tetramers. Data analysis was performed using FlowJo version 9.9.4 (TreeStar,
179 Ashland, OR). Statistical analyses were done using GraphPad Prism version 5 (La Jolla, CA).

180

181

182 **Statistical analyses:** Data for each assay were compared by analysis of variance (ANOVA)
183 and Student's *t*-test using GraphPad Prism version 5.03. ANOVA and multiple comparison procedures
184 identified differences between the groups, as we previously described in (21). Data are expressed as
185 the mean \pm SD. Results were considered statistically significant at $p < 0.05$.

186

187

RESULTS

188

189

1. *Composition of NK cell subsets in COVID-19 SYMP patients show a decreased*

190

CD56^{bright} NK cell population and higher frequency of mature/terminally differentiated NK cells

191

(CD57⁺) compared to Healthy individuals: NK cells are a subset of innate immune lymphocytes

192

composing 5% to 20% of PBMCs in humans and play an important role in the defense against viral

193

infections. These cells are reduced in numbers but less consistently than T cells, particularly in

194

severely sick patients. Therefore, we first investigated the phenotypic status of NK cells in SARS-

195

CoV-2 positive asymptomatic (ASYMP) and symptomatic (SYMP) patients and Healthy Controls. The

196

characteristics of the SYMP, ASYMP and Healthy control study populations used in this study,

197

concerning age, sex, HLA-A*02:01 frequency distribution, SARS-CoV-2 positivity, and status of

198

COVID-19 disease are presented in **Table 1**. These SARS-CoV-2 positive individuals were divided

199

into two groups: 1) HLA-A*02:01–positive SARS-CoV-2–infected ASYMP individuals, with no

200

detectable levels of any clinical COVID-19 disease; and 2) HLA-A*02:01–positive SARS-CoV-2–

201

infected SYMP individuals with a well-documented COVID-19 clinical disease.

202

We analyzed the NK cell population following a gating strategy as shown in **Fig. 1A**. The NK cell

203

population was further categorized into CD56^{dim} and CD56^{bright} cells, and their relative frequency was

204

evaluated in ASYMP, SYMP and Healthy individuals. Analysis of NK cell phenotype showed no

205

difference in mature CD56^{dim} subset in SARS-CoV-2 positive ASYMP and SYMP patients and Healthy

206

controls (**Fig. 1B, top panel**). However, SYMP patients significantly reduced immature CD56^{bright} NK

207

cells (**Fig. 1B, bottom panel; P = 0.02**) compared to Healthy controls.

208

CD57 expression on NK cells defines a mature phenotype, and their expression of CD57 could also

209

be considered a marker of terminal differentiation, although not associated with senescence in this

210

population. It is highly expressed on CD56^{dim} cells, representing mature NK cells, whereas less than

211

1% of CD56^{bright} NK cells, considered immature, also express CD57 (**Fig. 1C**). There was a significant

212 increase in the mature (CD56^{dim}/CD57⁺) and immature subset (CD56^{bright}/CD57⁺) (**Fig. 1C**, *top* and
213 *bottom panel*; $P = 0.03$ and $P = 0.01$ respectively) in SYMP patients with COVID-19 compared with
214 Healthy controls.

215 Collectively, these data indicate different states of maturation within the CD56^{dim} and
216 CD56^{bright} NK-cell subset and its correlation with COVID-19.

217

218 **2. The activation status, senescence, and exhaustion profile were significantly**
219 **increased in COVID-19 SYMP individuals compared to Healthy individuals within CD4⁺T cells:**

220 CD4⁺ T cells in COVID-19 are activated as characterized by the expression of cellular markers like
221 HLA-DR and CD38. Therefore, we next evaluated the degree of CD4⁺ T cell activation in COVID-19
222 positive ASYMP and SYMP patients and Healthy Controls. Within the CD4⁺ population, we analyzed
223 markers commonly related to T cell activation (HLA-DR and CD38). The gating strategy used to
224 analyze markers related to activation status, senescence, and exhaustion together within CD4⁺ T cells
225 is demonstrated in **Fig. 2A**. The expression of CD57 correlates with senescence in human CD4⁺ and
226 CD8⁺ T cells. Therefore, we compared the frequency of CD57⁺ on total CD4⁺T cells in COVID-19
227 ASYMP, SYMP and Healthy individuals. PBMC-derived CD57⁺CD4⁺ T cells detected from COVID-19
228 SYMP individuals showed an increased frequency compared to Healthy individuals (**Fig. 2B**; $P =$
229 0.03).

230 The levels of CD4⁺T-cell activation were also evaluated in SARS-CoV-2 infected ASYMP, SYMP
231 patients, and healthy controls. We found an increasing trend reflected by higher proportions of HLA-
232 DR⁺CD38⁺CD4⁺ T cells in SYMP patients compared to healthy controls, however with no statistical
233 significance (**Fig. 2C**).

234 Furthermore, we evaluated the expression of the senescence/exhaustion molecules on CD4⁺ T cells
235 by analyzing markers CD57 and PD-1 (**Fig. 2D**). The proportion of CD57⁺PD-1⁺CD4⁺ T cells was
236 significantly higher in COVID-19 positive SYMP patients than in healthy controls and ASYMP patients.

237 However, no statistical difference was detected in the proportion of CD57⁺PD-1⁺CD4⁺ T cells in
238 ASYMP and SYMP patients (**Fig. 2D**; $P = 0.03$).

239 Taken together, findings from COVID-19 positive SYMP individuals indicate the involvement of
240 activated CD4⁺ T cells and T cell exhaustion/senescence in the immunopathogenesis of SARS-CoV2
241 infection.

242 **3. Frequent SARS-CoV-2 specific senescent CD4⁺ T cells with an effector memory**
243 **phenotype (CD57⁺CD4⁺ T_{EM} and CD57⁺CD4⁺ T_{EMRA} cells) detected in COVID-19 SYMP individuals**
244 **compared to Healthy individuals:** SARS-CoV-2 specific memory CD4⁺ T cells were also
245 categorized into three major phenotypically distinct effector memory (TEM), central memory (TCM)
246 and a subset of effector memory T cells re-expresses CD45RA subpopulations termed as TEMRA.
247 Moreover, we studied the expression levels of CD57 on the memory CD4⁺ T cell subpopulations at
248 various stages of differentiation: central memory T cells, (CD45RA^{low}CCR7^{high}CD4⁺ T_{CM} cells); effector
249 memory T cells, (CD45RA^{low}CCR7^{low}CD4⁺ T_{EM} cells) and TEMRA T cells (CD45RA^{high}CCR7^{low}CD4⁺
250 T_{EMRA} cells). In the peripheral blood of HLA-A*02:01 positive, SARS-CoV-2 positive ASYMP, SYMP
251 and Healthy individuals, we compared the CD57 expression in CD4⁺ T cells and divided them into
252 T_{NAIVE}, T_{CM}, T_{EM}, and T_{EMRA} phenotypes (**Fig. 3A**). Similar percentages of
253 CD57⁺CD45RA^{low}CCR7^{high}CD4⁺ T_{CM} cells were detected in ASYMP, SYMP and Healthy individuals
254 (**Fig. 3B**; *left and right* panel). There was an increase in the CD57⁺CD45RA^{low}CCR7^{low}CD4⁺ T_{EM} cells
255 in SYMP individuals compared to Healthy controls (**Fig. 3C**; *left and right* panel ($P=0.02$)).
256 Significantly higher percentages of CD57⁺CD45RA^{high}CCR7^{low}CD4⁺ T_{EMRA} cells (**Fig. 3D**; *left and right*
257 panel) were detected in SYMP individuals compared to Healthy individuals ($P = 0.01$). Altogether, the
258 phenotypic properties of SARS-CoV-2 specific memory CD4⁺ T cells revealed a clear dichotomy in
259 memory CD4⁺ T cell sub-populations in SYMP versus Healthy individuals. SYMP individuals appeared
260 to develop frequent effector memory CD57⁺CD4⁺ T_{EMRA} and CD57⁺CD4⁺ T_{EM} cells compared to
261 Healthy and ASYMP individuals. By maintaining high frequencies of the SARS-CoV-2-specific

262 CD57⁺CD4⁺ T_{EMRA} cells and CD57⁺CD4⁺ T_{EM} cells, the SYMP individuals may not be protected against
263 infection and/or COVID-19 disease.

264

265 **4. Frequent SARS-COV-2 S₁₂₂₀₋₁₂₂₈ and S₉₅₈₋₉₆₆ epitope-specific CD57⁺CD8⁺T cells**

266 **detected in COVID-19 SYMP individuals compared to ASYMP and Healthy individuals:** As

267 described earlier SARS-CoV-2 positive individuals were segregated into two groups: 1) HLA-A*02:01–

268 positive SARS-CoV-2–infected ASYMP individuals, and 2) HLA-A*02:01–positive SARS-CoV-2–

269 infected SYMP individuals with a well-documented COVID-19 clinical disease. We next compared the

270 frequency of CD57⁺ on total CD8⁺T cells in HLA-A*02:01 positive COVID-19 ASYMP, SYMP and

271 Healthy individuals. We have used a gating strategy to analyze markers related to senescence

272 (CD57⁺) gated within CD8⁺ T cells from COVID-19 ASYMP, SYMP and Healthy individuals. Average

273 frequencies of PBMC-derived CD57⁺CD8⁺ T cells detected from COVID-19 SYMP individuals showed

274 an increased frequency compared to Healthy individuals (**Fig. 4A**, $P = 0.03$). We then compared the

275 frequency of SARS-CoV-2 peptide/tetramer complex specific CD8⁺T cells. The representative dot

276 plots in **Fig. 4B** indicate an increased frequency of CD57⁺CD8⁺ T cells, specific to S1220-1228

277 epitope in COVID-19 SYMP individuals compared to ASYMP Healthy individuals ($P = 0.01$). Similarly,

278 **Fig. 4C** depicts the high frequencies of CD57⁺CD8⁺ T cells detected in COVID-19 SYMP individuals

279 against another peptide/tetramer complex S₉₅₈₋₉₆₆ epitope ($P = 0.02$). Altogether, these results indicate

280 that SYMP individuals develop frequent SARS-CoV-2-specific CD57⁺CD8⁺ T cells compared to

281 ASYMP and Healthy individuals.

282

283 **5. Frequent SARS-CoV-2 S₁₂₂₀₋₁₂₂₈ epitope-specific senescent CD8⁺ T cells with an**

284 **effector memory phenotype (CD57⁺CD8⁺ T_{EM} and CD57⁺CD8⁺ T_{EMRA} cells) detected in COVID-19**

285 **SYMP individuals compared to Healthy individuals:** Similar to the CD4⁺T cell memory response,

286 SARS-CoV-2 specific memory CD8⁺ T cells are also categorized into three major phenotypically

287 distinct effector memory (TEM), central memory (TCM) and a subset of effector memory T cells re-

288 expresses CD45RA subpopulations termed as TEMRA. Furthermore, we examined the expression
289 levels of CD57 on the memory CD8⁺ T cell subpopulations at various stages of differentiation: central
290 memory T cells, (CD45RA^{low}CCR7^{high}CD8⁺ T_{CM} cells); effector memory T cells,
291 (CD45RA^{low}CCR7^{low}CD8⁺ T_{EM} cells) and TEMRA T cells (CD45RA^{high}CCR7^{low}CD8⁺ T_{EMRA} cells). In the
292 peripheral blood of HLA-A*02:01 positive, SARS-CoV-2 positive ASYMP, SYMP and Healthy
293 individuals, we compared the CD57 expression in CD8⁺ T cells specific to S₁₂₂₀₋₁₂₂₈ epitope and
294 divided them into T_{NAIVE}, T_{CM}, T_{EM}, and T_{EMRA} phenotypes (**Fig. 5A**). Similar percentages of
295 CD57⁺CD45RA^{low}CCR7^{high}CD8⁺ T_{CM} cells were detected in ASYMP, SYMP and Healthy individuals
296 (**Fig. 5B**; *left* and *right* panel). There was a significant increase in the CD57⁺CD45RA^{low}CCR7^{low}CD8⁺
297 T_{EM} cells in SYMP individuals compared to Healthy controls (**Fig. 5C**; *left* and *right* panel).
298 Significantly higher percentages of CD57⁺CD45RA^{high}CCR7^{low}CD8⁺ T_{EMRA} cells (**Fig. 5D**; *left* and *right*
299 panel) were detected in SYMP individuals compared to Healthy individuals ($P = 0.004$). Altogether,
300 the phenotypic properties of SARS-CoV-2 specific S₁₂₂₀₋₁₂₂₈ epitope epitope-specific memory CD8⁺ T
301 cells revealed a clear dichotomy in memory CD8⁺ T cell sub-populations in SYMP versus Healthy
302 individuals. SYMP individuals appeared to develop frequent SARS-CoV-2 specific effector memory
303 CD57⁺CD8⁺ T_{EMRA} and CD57⁺CD8⁺ T_{EM} cells compared to Healthy and ASYMP individuals. By
304 maintaining high frequencies of the SARS-CoV-2-specific CD57⁺CD8⁺ T_{EMRA} cells and CD57⁺CD8⁺
305 T_{EM} cells, the SYMP individuals may not be protected against infection and/or COVID-19 disease.

306

307 **6. The activation status, senescence, and exhaustion profile were significantly**
308 **increased in COVID-19 SYMP individuals compared to Healthy individuals within CD8⁺ T cells:**

309 Most viral infections induce activation of CD8⁺T cells that can be detected by increases in the co-
310 expression of CD38 and Human leukocyte antigen-DR isotype (HLA-DR). HLA-DR is constitutively
311 expressed by antigen-presenting cells (APCs) and is involved in the presentation of antigens to T-
312 cells. Most T-cells do not express it, but notably, a subset of activated T-cells becomes HLA-DR⁺
313 during an immune response. In contrast, CD38 is constitutively expressed by naive T-cells, down-

314 regulated in resting memory cells, and then elevated again in activated cells. Thus, we evaluated the
315 degree of CD8⁺ T-cell activation in COVID-19 positive ASYMP and SYMP patients and Healthy
316 Controls. Within the CD8⁺ population, we analyzed markers commonly related to T cell activation
317 (HLA-DR and CD38). Our gating strategy was used to analyze markers related to activation status,
318 senescence, and exhaustion together within SARS-CoV-2 specific CD8⁺ T cells (**Fig. 6A**). The levels
319 of T-cell activation were significantly higher (hyperactivated) in SARS-CoV-2 infected SYMP patients
320 than in healthy controls, as reflected by higher proportions of HLA-DR⁺CD38⁺CD8⁺ T cells (**Fig. 6B**, P
321 = 0.02).

322 We evaluated the senescence/exhaustion molecules expression on circulating T cells by
323 analyzing markers CD57 and PD-1 (**Fig. 6C**). We found that the proportion of CD57⁺PD-1⁺CD8⁺ T
324 cells was significantly higher in COVID-19 positive SYMP patients than in Healthy controls and
325 ASYMP patients. Still, there was no statistical difference in the proportion of CD57⁺PD-1⁺CD8⁺ T cells
326 in ASYMP and SYMP patients (**Fig. 6C**, $P = 0.009$).

327 Taken together, findings from COVID-19 positive SYMP individuals indicate the involvement of
328 hyperactivated CD8⁺T cells and T cell exhaustion/senescence in the immunopathogenesis of SARS-
329 CoV2 infection.

330

331 **7. Elevated Plasma levels of selective cytokines in COVID-19 ASYMP and SYMP**

332 **individuals compared to Healthy controls:** Many studies have previously reported that hyper-
333 inflammatory response induced by SARS-CoV-2 is a major cause of disease severity and death.
334 Therefore, we implemented a multiplex cytokine assay (Luminex) to measure inflammatory cytokines
335 known to contribute to pathogenic inflammation (IL)-6, IL-8, tumor necrosis factor (TNF)- α , interferon
336 (IFN)- γ and IL-17. in the plasma samples of COVID-19 in ASYMP, SYMP and Healthy individuals. The
337 cytokines assessed in this study had different detection ranges, with IL-6 and IL-8 having the most
338 dynamic profile followed by TNF- α , IL-17, and IFN- γ . We found that TNF- α and IFN- γ ($P = 0.001$) were

339 significantly elevated in COVID-19 symptomatic patients compared to Healthy controls (**Fig. 7A** and
340 **7B**). Similarly, we found that IL-6 and IL-8 ($P=0.01$) were significantly elevated in COVID-19
341 symptomatic patients compared to Healthy controls (**Fig. 7C** and **7D**). Interleukin (IL)-17 is one of the
342 many cytokines released during SARS-CoV-2 infection. IL-17 plays a crucial role in neutrophil
343 recruitment and activation. Neutrophils subsequently can migrate to the lung and are heavily involved
344 in the pathogenesis of COVID-19. We found that SARS-CoV-2 positive ASYMP and SYMP individuals
345 had significantly higher levels of IL-17 than Healthy controls ($P=0.04$) (**Fig. 7E**).
346 The vast majority of SYMP patients demonstrated elevated cytokines or cytokine storm compared to
347 Healthy controls. In contrast, the cytokine levels were not significantly different in COVID-19 ASYMP
348 and SYMP individuals.

349 Overall, our findings report that NK, CD4⁺ T cells, and CD8⁺ T cells' phenotypic and functional
350 characteristics in severe COVID-19 infection were compatible with activation of
351 dysfunction/exhaustion pathways.

352

353

354

355

356

357

358

359

360

361

362

363

364

365

366

367

368

369

370

DISCUSSION

371

372 COVID-19 is characterized by enhanced lymphopenia in the peripheral blood and altered T
373 cells phenotypes shown by a spectrum of activation and exhaustion. However, antigen-specific T cell
374 responses are emerging as a critical mechanism for both virus clearance and the most plausible
375 pathway to long-term immunological memory that would protect against re-infection. As a result, T cell
376 responses are of great importance in the development of vaccines (22). Moreover, post-infection
377 changes in the composition and function of T cell subsets have significant ramifications on the
378 patients' long-term immunological functions (23). The impairment of effector T cell responses has
379 been associated with the overexpression of inhibitory and senescent markers on T cells. Therefore,
380 the main objective of this research study was to detect T-cell immune signatures in peripheral blood,
381 including those of innate cells, and to determine how important indicators of activation and exhaustion
382 are related to the development of symptomatic COVID-19. Factors influencing the formation and
383 nature of protective immunity and severity of COVID-19 are still unknown. Nevertheless, data defining
384 disease phenotypes have the prospect of informed development of new therapeutic approaches for
385 treating individuals infected with SARS-CoV-2 and developing novel vaccines. CD57 is a marker on
386 some cell subsets, including T cells (15, 24, 25). A costimulatory molecule like CD28 (that provides
387 signaling for T cell activation) is expressed by naïve T cells after antigen recognition that may bind to
388 B7 proteins to provide co-stimulatory signals (26-28). However, repeated T-cell stimulation and
389 activation leads to gradual loss of CD28, a distinct characteristic of memory or terminally differentiated

390 cells, and subsequent upregulation of CD57 (29-31). These senescent cells are characterized by loss
391 of CD27 and display low proliferative capacity of the cells (32), eventually leading to an inability to
392 eradicate infection.

393 The CD57 antigen is commonly used to identify populations of late-differentiated 'senescent'
394 cells with defined cell phenotypes and effector functions (33, 34). In this report, we examined the
395 patterns of expression of CD57 on NK cells and SARS-CoV-2-specific T-cells and determined
396 increased expression of these exhaustive and senescent markers in symptomatic individuals
397 compared to those with asymptomatic infections and Healthy controls. While CD57 is now well-
398 recognized as a marker for terminally differentiated T-cells, it was originally thought to identify cells
399 with natural killer activity. The expression of CD57 varies among NK cell subsets. NK cells are innate
400 effector lymphocytes that respond to acute viral infections but might also contribute to
401 immunopathology. NK cells are typically divided into CD56^{bright} NK cells and CD56^{dim} NK cells, which
402 rapidly respond during diverse acute viral infections in humans, including against dengue virus,
403 hantavirus, tick-borne encephalitis virus, and yellow fever virus, among others (35-37). Although a
404 similar analysis of NK cells has not been performed in acute SARS-CoV-2 infection-causing COVID-
405 19, early reports from the pandemic (in line with our findings) have indicated low circulating NK cell
406 numbers in patients with moderate and severe disease (38-40). The SARS-CoV-2 infection has also
407 been linked to reduced NK cell counts during the acute phase of infection. We determined a terminally
408 differentiated phenotype with up-regulated levels of CD57 molecules in NK cells from SYMP COVID-
409 19 patients.

410 CD57 is expressed by CD16^{pos}CD56^{dim} cytotoxic NK cells and CD16^{pos}CD56^{neg} inflammatory
411 NK cells, whereas CD16^{neg}CD56^{bright} regulatory NK cells do not express this marker even during
412 chronic infections (41-43). The acquisition of CD57 thus follows the natural differentiation of NK cells
413 (from regulatory to cytotoxic to inflammatory NK cells). Thus, like T cells, NK cell expression of CD57

414 could be considered a marker of terminal differentiation, albeit not associated with senescence in this
415 population.

416 The majority of prior studies into the biology of CD57 focused on the antigen's significance in
417 distinct T cell subsets. In the late phases of differentiation, CD57 has been found both on CD4 and
418 CD8 T cells (15). CD57 identifies terminally differentiated cells with decreased proliferative responses
419 in CD8 T lymphocytes. T cell senescent markers were more associated with CD8⁺ T cells than CD4⁺T
420 cells, consistent with our results that accumulate at lower frequencies for CD4⁺T cells in the human
421 periphery (44). Our findings herein indicate an increased expression of CD57⁺T cell subsets in
422 symptomatic patients. It was previously shown that PD-1⁺CD57⁺CD8⁺T cells had increased sensitivity
423 to apoptosis mediated by PD-1 (45).

424 The increased expression of CD57 and PD-1 double-positive markers on CD8⁺ T cells in
425 COVID-19 suggests that these cells are at a higher risk of apoptosis. The fraction of T cells that
426 express CD57 increased in the symptomatic individuals, suggesting that the observed phenotypic
427 changes may lower the T cell repertoire's responsiveness to SARS-CoV-2 antigens, resulting in an
428 impaired ability to eliminate the infection. CD57⁺ memory T cells accumulate in peripheral blood
429 throughout life, especially after infection with CMV (46). These associations with age and persistent
430 antigenic drive were mechanistically linked in an *in vitro* study, which reported that replicative
431 senescent memory CD8⁺ T cells expressed CD57 (15). However, an earlier study had reached a
432 different conclusion (47), and later experiments showed that CD57⁺ memory CD8⁺ T cells could
433 proliferate *in vitro* in the presence of certain growth factors, potentially mimicking the *in vivo*
434 microenvironment (48). Recent studies suggest that TEMRA cells are fairly resistant to apoptosis and
435 remain in the CD8⁺ lineage for an estimated half-life of about 25 years, assuming simple exponential
436 decline without phenotypic change (49, 50). CD8⁺ TEMRA cells that expressed CD57 were recently
437 reported to be more sensitive to cell death than CD8⁺ TEMRA cells that lacked CD57 in response to
438 severe stimulation with supraphysiological doses of phytohemagglutinin and interleukin-2 (51).

439 Compared to asymptomatic individuals and Healthy controls, symptomatic patients had increased
440 CD57 expression on CD8⁺ TEMRA⁺ memory cells. Compared to asymptomatic infections, the
441 phenotypic abnormality of T cells during COVID-19 infections is more apparent in symptomatic
442 individuals and is associated with higher expression levels of exhaustive and senescent markers.

443 The findings of this research contribute to the current knowledge of the innate and adaptive
444 immune landscape in asymptomatic and symptomatic COVID-19 patients. However, we recognize
445 limitations that could be addressed with bigger sample numbers and matched control groups.
446 Furthermore, the phenotype and activity of immune cells from the lungs performing a direct role in
447 establishing symptomatic infections, are unknown. As a result, the immunophenotypic traits in the
448 lungs may not completely mirror the hierarchy of immunodominant circulating immune cells in the
449 blood.

450 In conclusion, this study presents an in-depth analysis of NK and T cell phenotypic and
451 functional characteristics that are associated with COVID-19 severe disease. The finding will inform
452 future immunotherapies to alleviate the symptoms of severe COVID-19 severe disease.

453

454

ACKNOWLEDGEMENTS

455 This work is supported by the Fast-Grant PR12501 from Emergent Ventures, a grant from
456 Herbert Family Trust, by Public Health Service Research grants AI158060, AI150091, and AI143348,
457 AI147499, AI143326, AI138764, AI124911 and AI110902 from the National Institutes of Allergy and
458 Infectious Diseases (NIAID) to LBM.

459 The authors would like to thank Dr. Dale Long from the NIH Tetramer Facility (Emory
460 University, Atlanta, GA) for providing the Tetramers used in this study. We thank UC Irvine Center for
461 Clinical Research (CCR) and Institute for Clinical & Translational Science (ICTS) for providing human
462 blood samples used in this study. A special thanks to Dr. Delia F. Tifrea for her continuous efforts and
463 dedication in providing COVID-19 samples that are crucial for this clinical research. We also thank
464 those who contributed directly or indirectly to this COVID-19 vaccine project: Dr. Steven A. Goldstein,
465 Dr. Michael J. Stamos, Dr. Suzanne B. Sandmeyer, Jim Mazzo, Dr. Daniela Bota, Dr. Beverly L.
466 Alger, Dr. Dan Forthal, Dr. Tahseen Muzaffar, Dr. Ilhem Messaoudi, Anju Subba, Janice Briggs,
467 Marge Brannon, Beverley Alberola, Jessica Sheldon, Rosie Magallon, and Andria Pontello.

468

469

REFERENCE

- 470 1. **Dong E, Du H, Gardner L.** 2020. An interactive web-based dashboard to track COVID-19 in
471 real time. *Lancet Infect Dis* **20**:533-534.
- 472 2. **Wu Z, McGoogan JM.** 2020. Characteristics of and Important Lessons From the Coronavirus
473 Disease 2019 (COVID-19) Outbreak in China: Summary of a Report of 72314 Cases From the
474 Chinese Center for Disease Control and Prevention. *JAMA* **323**:1239-1242.
- 475 3. **Benhadou F, Del Marmol V.** 2020. Improvement of SARS-CoV-2 symptoms following
476 Guselkumab injection in a psoriatic patient. *J Eur Acad Dermatol Venereol* **34**:e363-e364.
- 477 4. **Liguori C, Pierantozzi M, Spanetta M, Sarmati L, Cesta N, Iannetta M, Ora J, Mina GG,
478 Puxeddu E, Balbi O, Pezzuto G, Magrini A, Rogliani P, Andreoni M, Mercuri NB.** 2020.
479 Subjective neurological symptoms frequently occur in patients with SARS-CoV2 infection.
480 *Brain Behav Immun* **88**:11-16.
- 481 5. **Al-Tawfiq JA, Al-Homoud AH, Memish ZA.** 2020. Remdesivir as a possible therapeutic
482 option for the COVID-19. *Travel Med Infect Dis* **34**:101615.
- 483 6. **Breslin N, Baptiste C, Miller R, Fuchs K, Goffman D, Gyamfi-Bannerman C, D'Alton M.**
484 2020. Coronavirus disease 2019 in pregnancy: early lessons. *Am J Obstet Gynecol MFM*
485 **2**:100111.
- 486 7. **Moriyama M, Hugentobler WJ, Iwasaki A.** 2020. Seasonality of Respiratory Viral Infections.
487 *Annu Rev Virol* **7**:83-101.
- 488 8. **Neher RA, Dyrda R, Druelle V, Hodcroft EB, Albert J.** 2020. Potential impact of seasonal
489 forcing on a SARS-CoV-2 pandemic. *Swiss Med Wkly* **150**:w20224.
- 490 9. **Nishiura H, Linton NM, Akhmetzhanov AR.** 2020. Serial interval of novel coronavirus
491 (COVID-19) infections. *Int J Infect Dis* **93**:284-286.
- 492 10. **Zhang R, Li Y, Zhang AL, Wang Y, Molina MJ.** 2020. Identifying airborne transmission as
493 the dominant route for the spread of COVID-19. *Proc Natl Acad Sci U S A* **117**:14857-14863.

- 494 11. **Song H, Josleyn N, Janosko K, Skinner J, Reeves RK, Cohen M, Jett C, Johnson R,**
495 **Blaney JE, Bollinger L, Jennings G, Jahrling PB.** 2013. Monkeypox virus infection of
496 rhesus macaques induces massive expansion of natural killer cells but suppresses natural
497 killer cell functions. *PLoS One* **8**:e77804.
- 498 12. **Zingaropoli MA, Nijhawan P, Carraro A, Pasculli P, Zuccala P, Perri V, Marocco R,**
499 **Kertusha B, Siccardi G, Del Borgo C, Curtolo A, Ajassa C, Iannetta M, Ciardi MR,**
500 **Mastroianni CM, Lichtner M.** 2021. Increased sCD163 and sCD14 Plasmatic Levels and
501 Depletion of Peripheral Blood Pro-Inflammatory Monocytes, Myeloid and Plasmacytoid
502 Dendritic Cells in Patients With Severe COVID-19 Pneumonia. *Front Immunol* **12**:627548.
- 503 13. **De Biasi S, Meschiari M, Gibellini L, Bellinazzi C, Borella R, Fidanza L, Gozzi L, Iannone**
504 **A, Lo Tartaro D, Mattioli M, Paolini A, Menozzi M, Milic J, Franceschi G, Fantini R,**
505 **Tonelli R, Sita M, Sarti M, Trenti T, Brugioni L, Cicchetti L, Facchinetti F, Pietrangelo A,**
506 **Clini E, Girardis M, Guaraldi G, Mussini C, Cossarizza A.** 2020. Marked T cell activation,
507 senescence, exhaustion and skewing towards TH17 in patients with COVID-19 pneumonia.
508 *Nat Commun* **11**:3434.
- 509 14. **Pinti M, Appay V, Campisi J, Frasca D, Fulop T, Sauce D, Larbi A, Weinberger B,**
510 **Cossarizza A.** 2016. Aging of the immune system: Focus on inflammation and vaccination.
511 *Eur J Immunol* **46**:2286-2301.
- 512 15. **Brenchley JM, Karandikar NJ, Betts MR, Ambrozak DR, Hill BJ, Crotty LE, Casazza JP,**
513 **Kuruppu J, Migueles SA, Connors M, Roederer M, Douek DC, Koup RA.** 2003. Expression
514 of CD57 defines replicative senescence and antigen-induced apoptotic death of CD8+ T cells.
515 *Blood* **101**:2711-20.
- 516 16. **Nielsen CM, White MJ, Goodier MR, Riley EM.** 2013. Functional Significance of CD57
517 Expression on Human NK Cells and Relevance to Disease. *Front Immunol* **4**:422.
- 518 17. **Pangrazzi L, Reidla J, Carmona Arana JA, Naismith E, Miggitsch C, Meryk A, Keller M,**
519 **Krause AAN, Melzer FL, Trieb K, Schirmer M, Grubeck-Loebenstien B, Weinberger B.**

- 520 2020. CD28 and CD57 define four populations with distinct phenotypic properties within
521 human CD8(+) T cells. *Eur J Immunol* **50**:363-379.
- 522 18. **van Deursen JM**. 2014. The role of senescent cells in ageing. *Nature* **509**:439-46.
- 523 19. **Prakash S, Srivastava R, Coulon PG, Dhanushkodi NR, Chentoufi AA, Tifrea DF,**
524 **Edwards RA, Figueroa CJ, Schubl SD, Hsieh L, Buchmeier MJ, Bouziane M, Nesburn**
525 **AB, Kuppermann BD, BenMohamed L**. 2021. Genome-Wide B Cell, CD4(+), and CD8(+) T
526 Cell Epitopes That Are Highly Conserved between Human and Animal Coronaviruses,
527 Identified from SARS-CoV-2 as Targets for Preemptive Pan-Coronavirus Vaccines. *J Immunol*
528 **206**:2566-2582.
- 529 20. **Chentoufi AA, Zhang X, Lamberth K, Dasgupta G, Bettahi I, Nguyen A, Wu M, Zhu X,**
530 **Mohebbi A, Buus S, Wechsler SL, Nesburn AB, BenMohamed L**. 2008. HLA-A*0201-
531 restricted CD8+ cytotoxic T lymphocyte epitopes identified from herpes simplex virus
532 glycoprotein D. *J Immunol* **180**:426-37.
- 533 21. **Zhang X, Chentoufi AA, Dasgupta G, Nesburn AB, Wu M, Zhu X, Carpenter D, Wechsler**
534 **SL, You S, BenMohamed L**. 2009. A genital tract peptide epitope vaccine targeting TLR-2
535 efficiently induces local and systemic CD8+ T cells and protects against herpes simplex virus
536 type 2 challenge. *Mucosal Immunol* **2**:129-43.
- 537 22. **Shah VK, Fimal P, Alam A, Ganguly D, Chattopadhyay S**. 2020. Overview of Immune
538 Response During SARS-CoV-2 Infection: Lessons From the Past. *Front Immunol* **11**:1949.
- 539 23. **Nikolich-Zugich J**. 2008. Ageing and life-long maintenance of T-cell subsets in the face of
540 latent persistent infections. *Nat Rev Immunol* **8**:512-22.
- 541 24. **Strauss-Albee DM, Horowitz A, Parham P, Blish CA**. 2014. Coordinated regulation of NK
542 receptor expression in the maturing human immune system. *J Immunol* **193**:4871-9.
- 543 25. **Fletcher JM, Vukmanovic-Stejic M, Dunne PJ, Birch KE, Cook JE, Jackson SE, Salmon**
544 **M, Rustin MH, Akbar AN**. 2005. Cytomegalovirus-specific CD4+ T cells in healthy carriers are
545 continuously driven to replicative exhaustion. *J Immunol* **175**:8218-25.

- 546 26. **Effros RB.** 1997. Loss of CD28 expression on T lymphocytes: a marker of replicative
547 senescence. *Dev Comp Immunol* 21:471-8.
- 548 27. **Effros RB, Pawelec G.** 1997. Replicative senescence of T cells: does the Hayflick Limit lead
549 to immune exhaustion? *Immunol Today* 18:450-4.
- 550 28. **Harding FA, McArthur JG, Gross JA, Raulet DH, Allison JP.** 1992. CD28-mediated
551 signalling co-stimulates murine T cells and prevents induction of anergy in T-cell clones.
552 *Nature* 356:607-9.
- 553 29. **Li G, Larregina AT, Domsic RT, Stolz DB, Medsger TA, Jr., Lafyatis R, Fuschiotti P.** 2017.
554 Skin-Resident Effector Memory CD8(+)CD28(-) T Cells Exhibit a Profibrotic Phenotype in
555 Patients with Systemic Sclerosis. *J Invest Dermatol* 137:1042-1050.
- 556 30. **Yu HT, Park S, Shin EC, Lee WW.** 2016. T cell senescence and cardiovascular diseases.
557 *Clin Exp Med* 16:257-63.
- 558 31. **Kaplan RC, Sinclair E, Landay AL, Lurain N, Sharrett AR, Gange SJ, Xue X, Hunt P,
559 Karim R, Kern DM, Hodis HN, Deeks SG.** 2011. T cell activation and senescence predict
560 subclinical carotid artery disease in HIV-infected women. *J Infect Dis* 203:452-63.
- 561 32. **Olsson J, Wikby A, Johansson B, Lofgren S, Nilsson BO, Ferguson FG.** 2000. Age-
562 related change in peripheral blood T-lymphocyte subpopulations and cytomegalovirus infection
563 in the very old: the Swedish longitudinal OCTO immune study. *Mech Ageing Dev* 121:187-
564 201.
- 565 33. **Neidleman J, Luo X, Frouard J, Xie G, Gill G, Stein ES, McGregor M, Ma T, George AF,
566 Kosters A, Greene WC, Vasquez J, Ghosn E, Lee S, Roan NR.** 2020. SARS-CoV-2-Specific
567 T Cells Exhibit Phenotypic Features of Helper Function, Lack of Terminal Differentiation, and
568 High Proliferation Potential. *Cell Rep Med* 1:100081.
- 569 34. **Zhang J, He T, Xue L, Guo H.** 2021. Senescent T cells: a potential biomarker and target for
570 cancer therapy. *EBioMedicine* 68:103409.

- 571 35. **Bjorkstrom NK, Lindgren T, Stoltz M, Fauriat C, Braun M, Evander M, Michaelsson J,**
572 **Malmberg KJ, Klingstrom J, Ahlm C, Ljunggren HG.** 2011. Rapid expansion and long-term
573 persistence of elevated NK cell numbers in humans infected with hantavirus. *J Exp Med*
574 **208**:13-21.
- 575 36. **Zimmer CL, Cornillet M, Sola-Riera C, Cheung KW, Ivarsson MA, Lim MQ, Marquardt N,**
576 **Leo YS, Lye DC, Klingstrom J, MacAry PA, Ljunggren HG, Rivino L, Bjorkstrom NK.**
577 2019. NK cells are activated and primed for skin-homing during acute dengue virus infection in
578 humans. *Nat Commun* **10**:3897.
- 579 37. **Blom K, Braun M, Pakalniene J, Lunemann S, Enqvist M, Dailidyte L, Schaffer M,**
580 **Lindquist L, Mickiene A, Michaelsson J, Ljunggren HG, Gredmark-Russ S.** 2016. NK Cell
581 Responses to Human Tick-Borne Encephalitis Virus Infection. *J Immunol* **197**:2762-71.
- 582 38. **Jiang Y, Wei X, Guan J, Qin S, Wang Z, Lu H, Qian J, Wu L, Chen Y, Chen Y, Lin X.** 2020.
583 COVID-19 pneumonia: CD8(+) T and NK cells are decreased in number but compensatory
584 increased in cytotoxic potential. *Clin Immunol* **218**:108516.
- 585 39. **Mazzoni A, Salvati L, Maggi L, Capone M, Vanni A, Spinicci M, Mencarini J, Caporale R,**
586 **Peruzzi B, Antonelli A, Trotta M, Zammarchi L, Ciani L, Gori L, Lazzeri C, Matucci A,**
587 **Vultaggio A, Rossi O, Almerigogna F, Parronchi P, Fontanari P, Lavorini F, Peris A,**
588 **Rossolini GM, Bartoloni A, Romagnani S, Liotta F, Annunziato F, Cosmi L.** 2020.
589 Impaired immune cell cytotoxicity in severe COVID-19 is IL-6 dependent. *J Clin Invest*
590 **130**:4694-4703.
- 591 40. **Wang F, Nie J, Wang H, Zhao Q, Xiong Y, Deng L, Song S, Ma Z, Mo P, Zhang Y.** 2020.
592 Characteristics of Peripheral Lymphocyte Subset Alteration in COVID-19 Pneumonia. *J Infect*
593 *Dis* **221**:1762-1769.
- 594 41. **Lopez-Verges S, Milush JM, Pandey S, York VA, Arakawa-Hoyt J, Pircher H, Norris PJ,**
595 **Nixon DF, Lanier LL.** 2010. CD57 defines a functionally distinct population of mature NK cells
596 in the human CD56dimCD16+ NK-cell subset. *Blood* **116**:3865-74.

- 597 42. **Bjorkstrom NK, Ljunggren HG, Sandberg JK.** 2010. CD56 negative NK cells: origin,
598 function, and role in chronic viral disease. *Trends Immunol* **31**:401-6.
- 599 43. **Bjorkstrom NK, Riese P, Heuts F, Andersson S, Fauriat C, Ivarsson MA, Bjorklund AT,**
600 **Flodstrom-Tullberg M, Michaelsson J, Rottenberg ME, Guzman CA, Ljunggren HG,**
601 **Malmberg KJ.** 2010. Expression patterns of NKG2A, KIR, and CD57 define a process of
602 CD56dim NK-cell differentiation uncoupled from NK-cell education. *Blood* **116**:3853-64.
- 603 44. **Valenzuela HF, Effros RB.** 2002. Divergent telomerase and CD28 expression patterns in
604 human CD4 and CD8 T cells following repeated encounters with the same antigenic stimulus.
605 *Clin Immunol* **105**:117-25.
- 606 45. **Petrovas C, Chaon B, Ambrozak DR, Price DA, Melenhorst JJ, Hill BJ, Geldmacher C,**
607 **Casazza JP, Chattopadhyay PK, Roederer M, Douek DC, Mueller YM, Jacobson JM,**
608 **Kulkarni V, Felber BK, Pavlakis GN, Katsikis PD, Koup RA.** 2009. Differential association
609 of programmed death-1 and CD57 with ex vivo survival of CD8+ T cells in HIV infection. *J*
610 *Immunol* **183**:1120-32.
- 611 46. **Gratama JW, Fridell E, Lenkei R, Oosterveer MA, Ljungstrom I, Tanke HJ, Linde A.** 1989.
612 Correlation between cytomegalovirus and toxoplasma gondii serology and lymphocyte
613 phenotypes in peripheral blood and cord blood. *Scand J Infect Dis* **21**:611-6.
- 614 47. **Izquierdo M, Balboa MA, Fernandez-Ranada JM, Figuera A, Torres A, Iriando A, Lopez-**
615 **Botet M.** 1990. Relation between the increase of circulating CD3+ CD57+ lymphocytes and T
616 cell dysfunction in recipients of bone marrow transplantation. *Clin Exp Immunol* **82**:145-50.
- 617 48. **Chong LK, Aicheler RJ, Llewellyn-Lacey S, Tomasec P, Brennan P, Wang EC.** 2008.
618 Proliferation and interleukin 5 production by CD8hi CD57+ T cells. *Eur J Immunol* **38**:995-
619 1000.
- 620 49. **Gupta S, Su H, Bi R, Agrawal S, Gollapudi S.** 2005. Life and death of lymphocytes: a role in
621 immunosenescence. *Immun Ageing* **2**:12.

- 622 50. **Ladell K, Hellerstein MK, Cesar D, Busch R, Boban D, McCune JM.** 2008. Central memory
623 CD8+ T cells appear to have a shorter lifespan and reduced abundance as a function of HIV
624 disease progression. *J Immunol* **180**:7907-18.
- 625 51. **Verma K, Ogonek J, Varanasi PR, Luther S, Bunting I, Thomay K, Behrens YL, Mischak-
626 Weissinger E, Hambach L.** 2017. Human CD8+ CD57- TEMRA cells: Too young to be called
627 "old". *PLoS One* **12**:e0177405.

628

629

630

631

FIGURE LEGENDS

632

633 **Figure 1: Composition of NK cell subsets in COVID-19 SYMP individuals shows a**
634 **decreased CD56^{bright} NK cell population and a higher frequency of mature/terminally**
635 **differentiated NK cells (CD57⁺) than in Healthy individuals.**

636 A gating strategy for defining of NK cell population is shown using FACS. **(A)** Using forward
637 scatter (FSC) and side scatters (SSC), the lymphocyte populations were gated. Singlets were gated
638 after gating the lymphocytes population, and NK cells were defined as CD3⁻ CD56⁺ cells. The NK cell
639 population was further categorized into CD56^{dim} and CD56^{bright} cells, and their relative frequency of
640 senescence (CD57⁺) was evaluated. **(B)** Representative FACS data of the frequencies of CD56^{dim} NK
641 cells and CD56^{bright} NK cells detected in PBMCs from COVID-19 ASYMP individuals SYMP individuals
642 and Healthy controls (*left panel*). Average frequencies of PBMC-derived CD56^{dim} NK cells (*top*) and
643 CD56^{bright} NK cells (*bottom*) were detected from ASYMP, SYMP and Healthy individuals (*right panel*).

644 **(C)** Representative FACS data of the frequencies of CD57 gated on CD56^{dim} NK cells and the
645 frequencies of CD57 gated on CD56^{bright} NK cells detected in PBMCs from COVID-19 ASYMP
646 individual, SYMP individual, and Healthy control (*left panel*). Average frequencies of PBMCs-derived

647 CD56^{dim} NK cells (*top*) and CD56^{bright} NK cells (*bottom*) were detected from ASYMP, SYMP and
648 Healthy individuals (*right panel*). The results are representative of two independent experiments on
649 each individual. The indicated *P* values, calculated using an unpaired t-test, show statistical
650 significance between SYMP and Healthy individuals.

651

652 **Figure 2: The activation status, senescence, and exhaustion profile were significantly**
653 **increased in COVID-19 SYMP individuals compared to Healthy individuals within CD4⁺ T cells.**

654 Expression of CD38 and HLA-DR was detected to analyze the activation status of CD4⁺ T
655 cells. Expression of CD57 and PD-1 was detected to analyze the senescence/exhaustion status of
656 CD4⁺ T cells. **(A)** The gating strategy was used to analyze markers related to activation status,
657 senescence, and exhaustion together within CD4⁺ T cells. Activated cells are CD38⁺HLA-DR⁺;
658 exhausted/senescent are PD1⁺CD57⁺. **(B)** Representative FACS data of the frequencies of CD57⁺
659 CD4⁺ T cells detected in PBMCs from COVID-19 ASYMP, SYMP and Healthy individuals (*left panel*).
660 Average frequencies of PBMC-derived CD57⁺ CD4⁺ T cells were detected from ASYMP, SYMP and
661 Healthy individuals (*right panel*). **(C)** Representative FACS data of the frequencies of HLA-DR⁺CD38⁺
662 CD4⁺ T cells detected in PBMCs from ASYMP individual, SYMP individual and Healthy control (*left*
663 *panel*). Average frequencies of PBMC-derived HLA-DR⁺CD38⁺ CD4⁺ T cells were detected from
664 ASYMP SYMP and Healthy individuals (*right panel*). **(D)** Representative FACS data of the frequencies
665 of CD57⁺ PD-1⁺CD4⁺ T cells detected in PBMCs from COVID-19 ASYMP, SYMP and Healthy
666 individuals (*left panel*). Average frequencies of PBMCs-derived CD57⁺ PD-1⁺CD4⁺ T cells were
667 detected from ASYMP, SYMP and Healthy individuals (*right panel*). The results are representative of
668 two independent experiments on each individual. The indicated *P* values, calculated using an
669 unpaired t-test, show statistical significance between SYMP and Healthy individuals.

670

671 **Figure 3: Frequent SARS-CoV-2 specific senescent CD4⁺ T cells with an effector memory**
672 **phenotype (CD57⁺CD4⁺ T_{EM} and CD57⁺CD4⁺ T_{EMRA} cells) detected in COVID-19 SYMP individuals**
673 **compared to Healthy individuals.**

674 The phenotype of CD4⁺ T cells and the gating strategy shown in **Fig. 2A** were analyzed in
675 T_{NAIVE}, T_{CM}, T_{EMRA}, and T_{EM} phenotypes in PBMCs from COVID-19 ASYMP SYMP and Healthy
676 individuals. Representative FACS data (*left panel*) and the frequencies of CD57 (*right panel*) (**B**)
677 gated on CD45RA^{low}CCR7^{high}CD4⁺ T_{CM} cells, (**C**) gated on CD45RA^{low}CCR7^{low}CD4⁺ T_{EM} cells, and (**D**)
678 and CD45RA^{high}CCR7^{low}CD4⁺ T_{EMRA} cells detected in COVID-19 ASYMP individual, SYMP individual
679 and Healthy individual. The results are representative of two independent experiments on each
680 individual. The indicated *P* values, calculated using an unpaired t-test, show statistical significance
681 between SYMP and Healthy individuals.

682

683 **Figure 4: Frequent SARS-COV-2 S₁₂₂₀₋₁₂₂₈ and S₉₅₈₋₉₆₆ epitope-specific CD57⁺CD8⁺ T cells**
684 **detected in COVID-19 SYMP individuals compared to ASYMP and Healthy individuals.**

685 The frequency of CD57⁺ on total CD8⁺ T cells and SARS-CoV-2 peptide/tetramer complex
686 specific CD8⁺T cells were analyzed in HLA-A*02:01 positive COVID-19 ASYMP, SYMP and Healthy
687 individuals. (**A**) Gating strategy used to analyze markers related to senescence gated within CD8⁺ T
688 cells from COVID-19 ASYMP, SYMP and Healthy individuals (*left panel*), and average frequencies of
689 PBMC-derived CD8⁺ T cells detected from COVID-19 ASYMP, SYMP and Healthy individuals (*right*
690 *panel*). (**B**) Representative FACS data of the frequencies of CD57⁺CD8⁺ T cells, specific to S₁₂₂₀₋₁₂₂₈
691 epitope, detected in PBMCs from HLA-A*02:01 positive COVID-19 ASYMP, SYMP and Healthy
692 individuals (*left panel*). Average frequencies of PBMC-derived CD8⁺ T cells, specific to S₁₂₂₀₋₁₂₂₈
693 epitope, were detected from COVID-19 ASYMP, SYMP and Healthy individuals (*right panel*). (**C**)
694 Representative FACS data of the frequencies of CD57⁺CD8⁺ T cells, specific to S₉₅₈₋₉₆₆ epitope,
695 detected in PBMCs from HLA-A*02:01 positive COVID-19 ASYMP, SYMP and Healthy individuals
696 (*left panel*). Average frequencies of PBMC-derived CD57⁺CD8⁺ T cells, specific to S₉₅₈₋₉₆₆ epitope,

697 were detected from ASYMP, SYMP and Healthy individuals (*right panel*). The results are
698 representative of two independent experiments on each individual. The indicated *P* values, calculated
699 using an unpaired t-test, show statistical significance between SYMP and Healthy individuals.

700

701 **Figure 5: Frequent SARS-CoV-2 S₁₂₂₀₋₁₂₂₈ epitope-specific senescent CD8⁺ T cells with an**
702 **effector memory phenotype (CD57⁺CD8⁺ T_{EM} and CD57⁺CD8⁺ T_{EMRA} cells) detected in COVID-19**
703 **SYMP individuals compared to Healthy individuals.**

704 The phenotype of CD8⁺ T cells specific to S₁₂₂₀₋₂₂₈ peptide/tetramer shown in **Fig. 5A** was
705 analyzed in terms of T_{NAIVE}, T_{CM}, T_{EMRA}, and T_{EM} phenotypes in PBMCs from HLA-A*02:01 positive
706 COVID-19 ASYMP, SYMP and Healthy individuals. Representative FACS data (*left panel*) and the
707 frequencies of CD57 (*right panel*) gated on CD45RA^{low}CCR7^{high}CD8⁺ T_{CM} cells (**B**), gated on
708 CD45RA^{low}CCR7^{low}CD8⁺ T_{EM} cells (**C**), and CD45RA^{high}CCR7^{low}CD8⁺ T_{EMRA} cells (**D**) detected in
709 COVID-19 ASYMP, SYMP and Healthy individuals. The results are representative of two independent
710 experiments on each individual. The indicated *P* values, calculated using an unpaired t-test, show
711 statistical significance between SYMP and Healthy individuals.

712

713 **Figure 6: The activation status, senescence, and exhaustion profile were significantly**
714 **increased in COVID-19 SYMP individuals compared to Healthy individuals within CD8⁺T cells.**

715 Expression of CD38 and HLA-DR was detected to analyze the activation status of CD8⁺ T
716 cells. Expression of CD57 and PD-1 was detected to analyze the senescence/exhaustion status of
717 CD8⁺ T cells. (**A**) Gating strategy used to analyze markers related to activation status, senescence,
718 and exhaustion together within SARS-CoV-2 specific CD8⁺ T cells. Activated cells are CD38⁺HLA-
719 DR⁺; exhausted/senescent are PD1⁺CD57⁺. FACS was used to determine the expression level of
720 various markers on tetramer gated CD8⁺ T cells specific to the S₁₂₂₀₋₁₂₂₈ epitope. (**B**) Representative
721 FACS data of the frequencies of HLA-DR⁺CD38⁺ CD8⁺ T cells, specific to S₁₂₂₀₋₁₂₂₈ epitope detected in
722 PBMCs from HLA-A*02:01 positive COVID-19 ASYMP individuals, SYMP individuals, and Healthy

723 controls (*left panel*). Average frequencies of PBMCs-derived HLA-DR⁺CD38⁺ CD8⁺ T cells, specific to
724 S₁₂₂₀₋₁₂₂₈ epitope, were detected from COVID-19 ASYMP, SYMP and Healthy individuals (*right panel*).
725 **(C)** Representative FACS data of the frequencies of CD57⁺ PD-1⁺CD8⁺ T cells, specific to S₁₂₂₀₋₁₂₂₈
726 epitope, detected in PBMCs from HLA-A*02:01 positive COVID-19 ASYMP individuals, SYMP
727 individuals, and Healthy individuals (*left panel*). Average frequencies of PBMCs-derived CD57⁺ PD-
728 1⁺CD8⁺ T cells, specific to the S₁₂₂₀₋₁₂₂₈ epitope, were detected from ASYMP, SYMP and Healthy
729 individuals (*right panel*). The results are representative of two independent experiments on each
730 individual. The indicated *P* values, calculated using an unpaired t-test, show statistical significance
731 between SYMP and Healthy individuals.

732

733

734 **Figure 7: Elevated Plasma levels of selective cytokines in COVID-19 ASYMP and SYMP**
735 **individuals compared to Healthy controls.**

736 Cytokine expression levels of two replicates per sample were measured in plasma samples of
737 COVID-19 ASYMP, SYMP and Healthy individuals using Luminex. **(A)** Bar graphs with individual
738 values showing the average amount of TNF- α (pg/ml) produced from ASYMP, SYMP and Healthy
739 individuals. **(B)** Bar graphs with individual values showing the average amount of IFN- γ (pg/ml)
740 produced from ASYMP, SYMP and Healthy individuals. **(C)** Bar graphs with individual values show
741 the average IL-6 (pg/ml) produced from ASYMP, SYMP and Healthy individuals. **(D)** Bar graphs with
742 individual values show the average IL-8 (pg/ml) produced from ASYMP, SYMP and Healthy
743 individuals. **(E)** Bar graphs with individual values show the average IL-17 (pg/ml) produced from
744 ASYMP, SYMP and Healthy individuals.

745

746

747

748

749

750

751

752

753

754

755

Fig. 1. Srivastava et al.

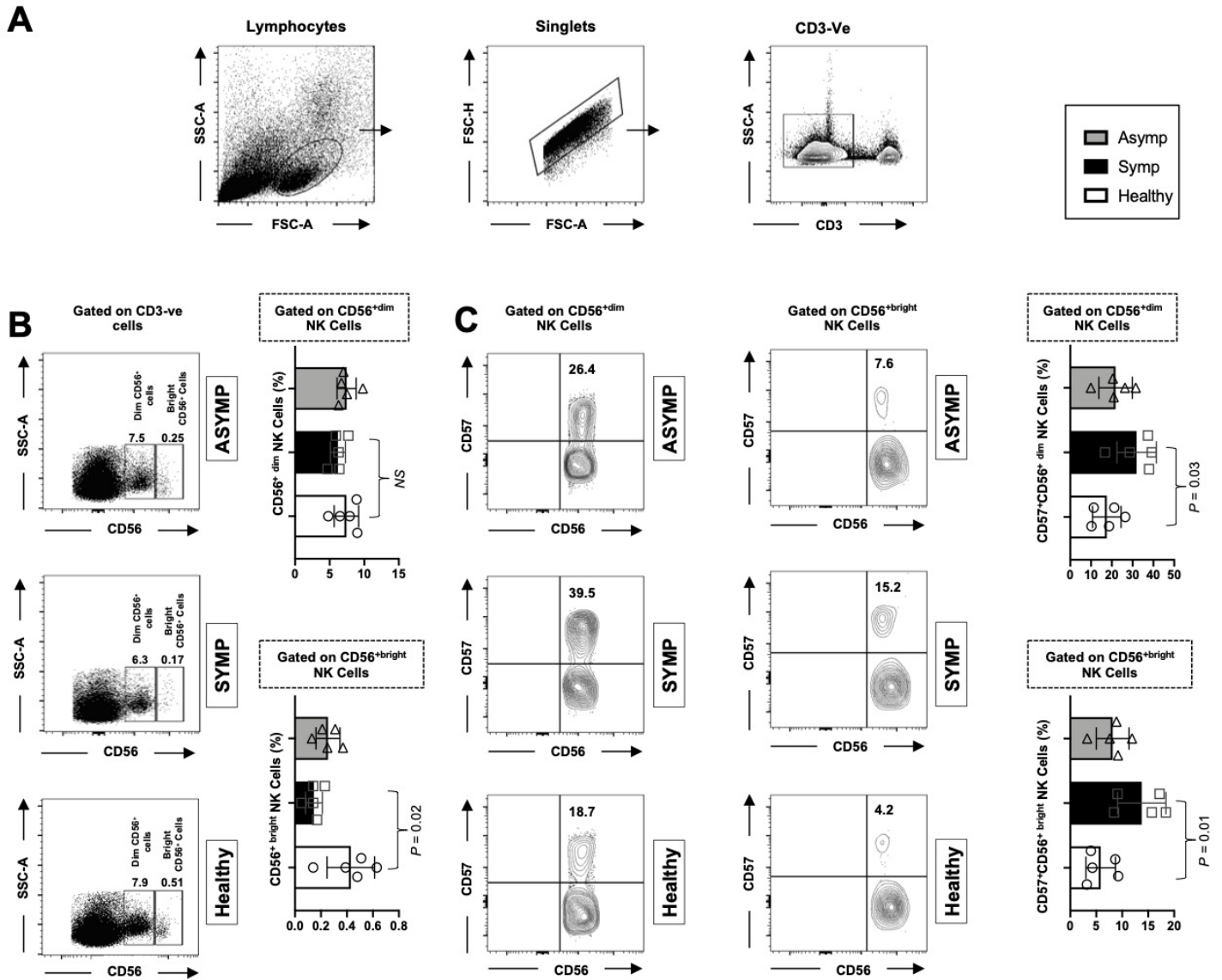


Fig. 2. Srivastava et al.

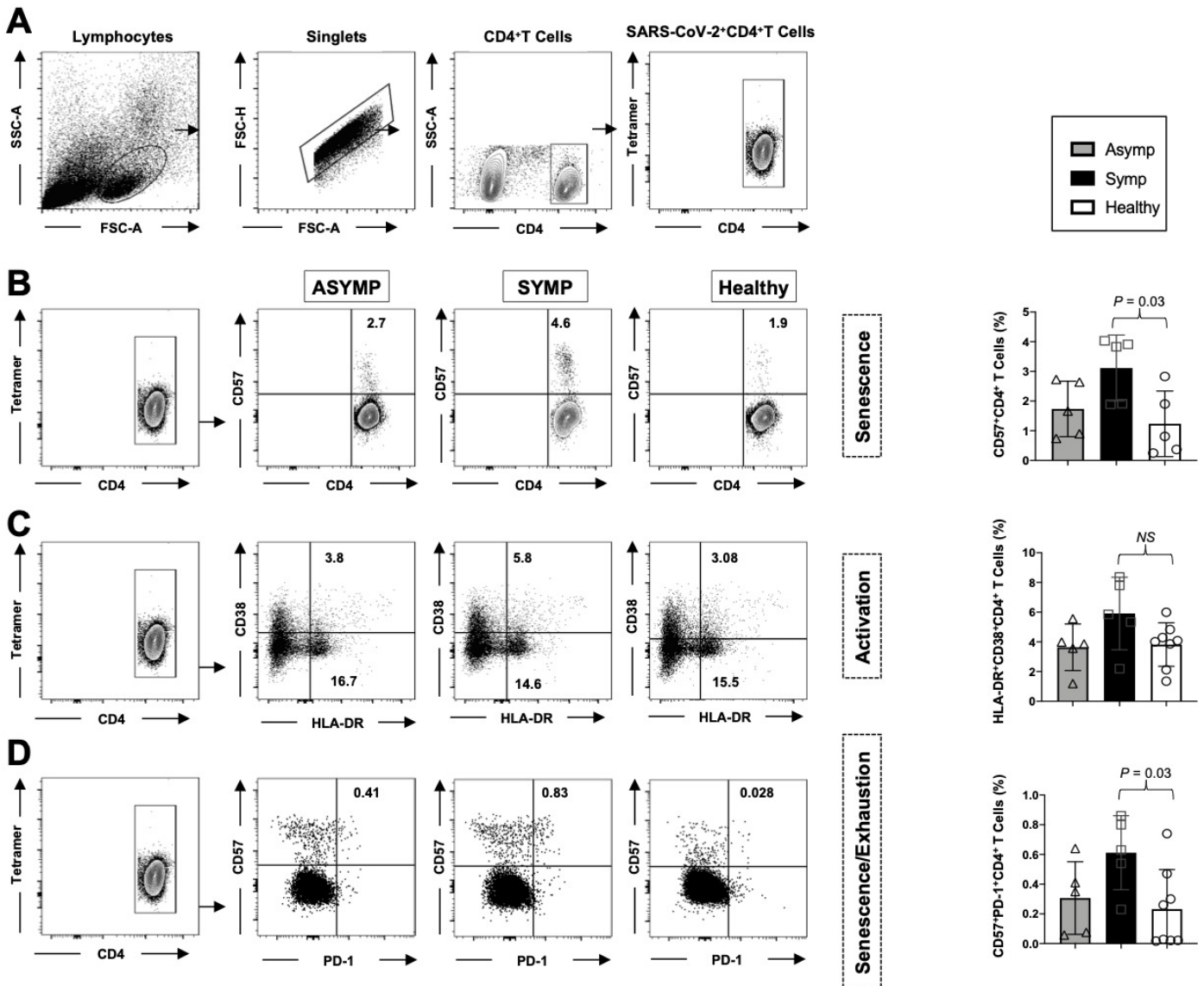


Fig. 3. Srivastava et al.

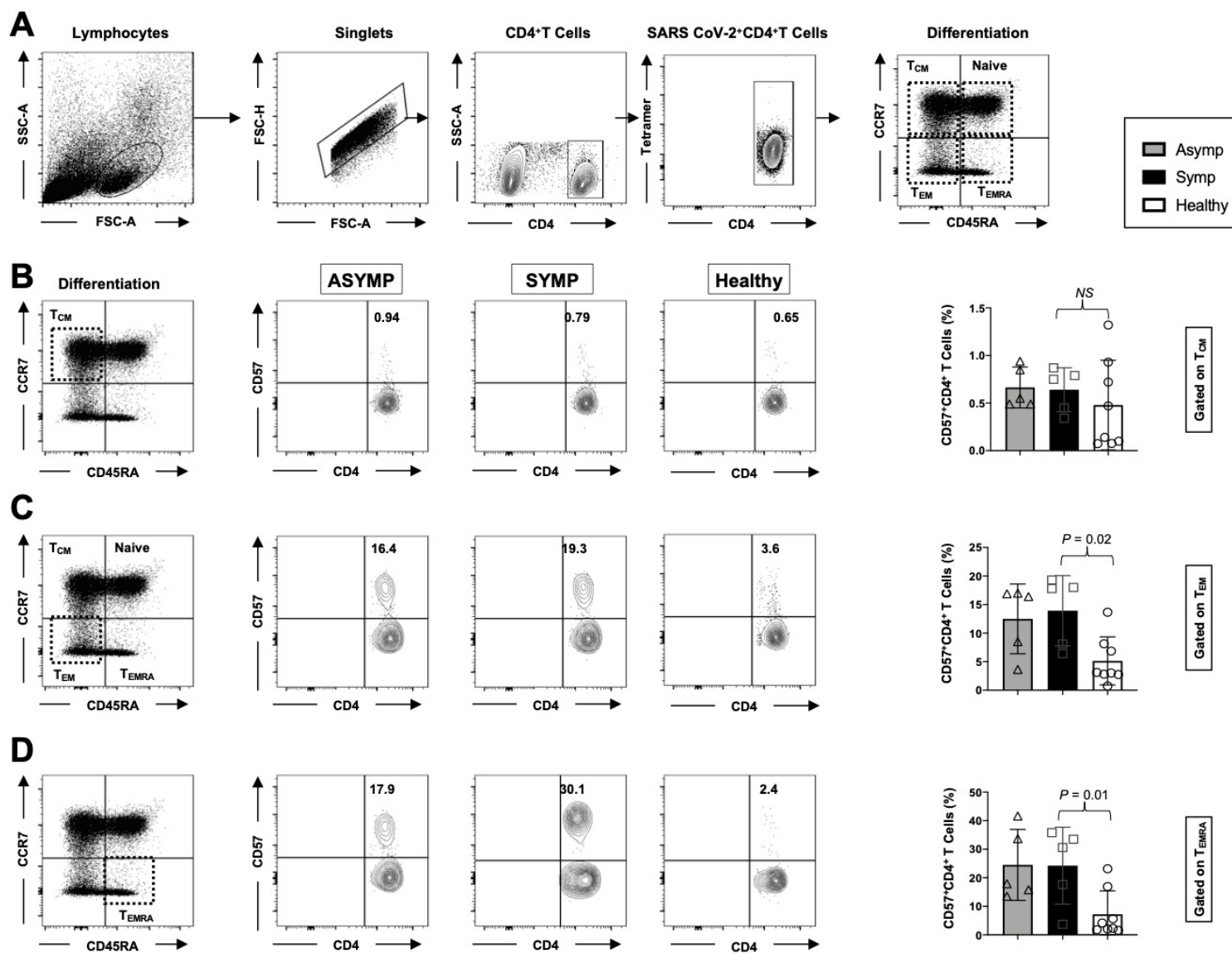


Fig. 4. Srivastava et al.

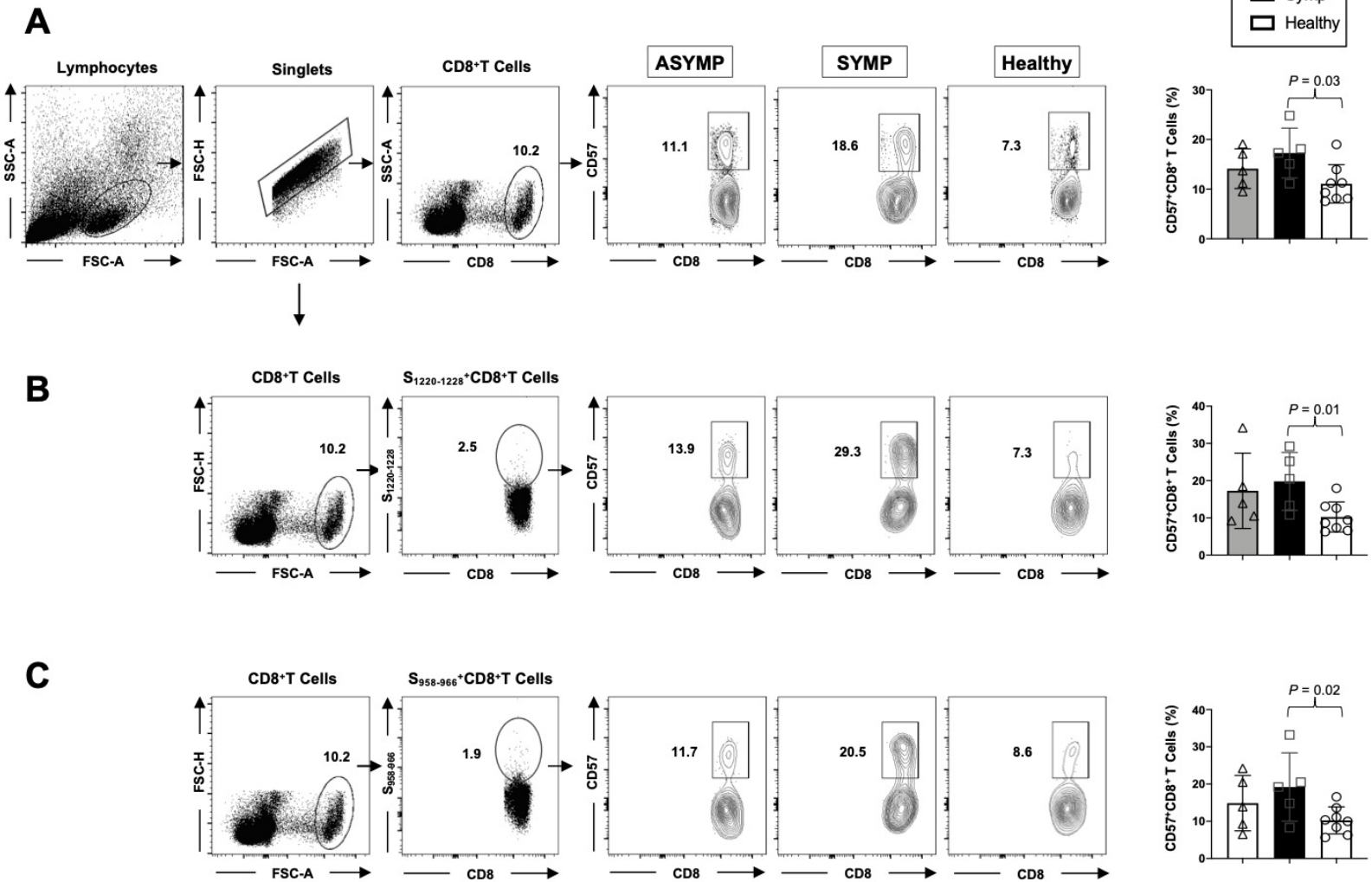


Fig. 5. Srivastava et al.

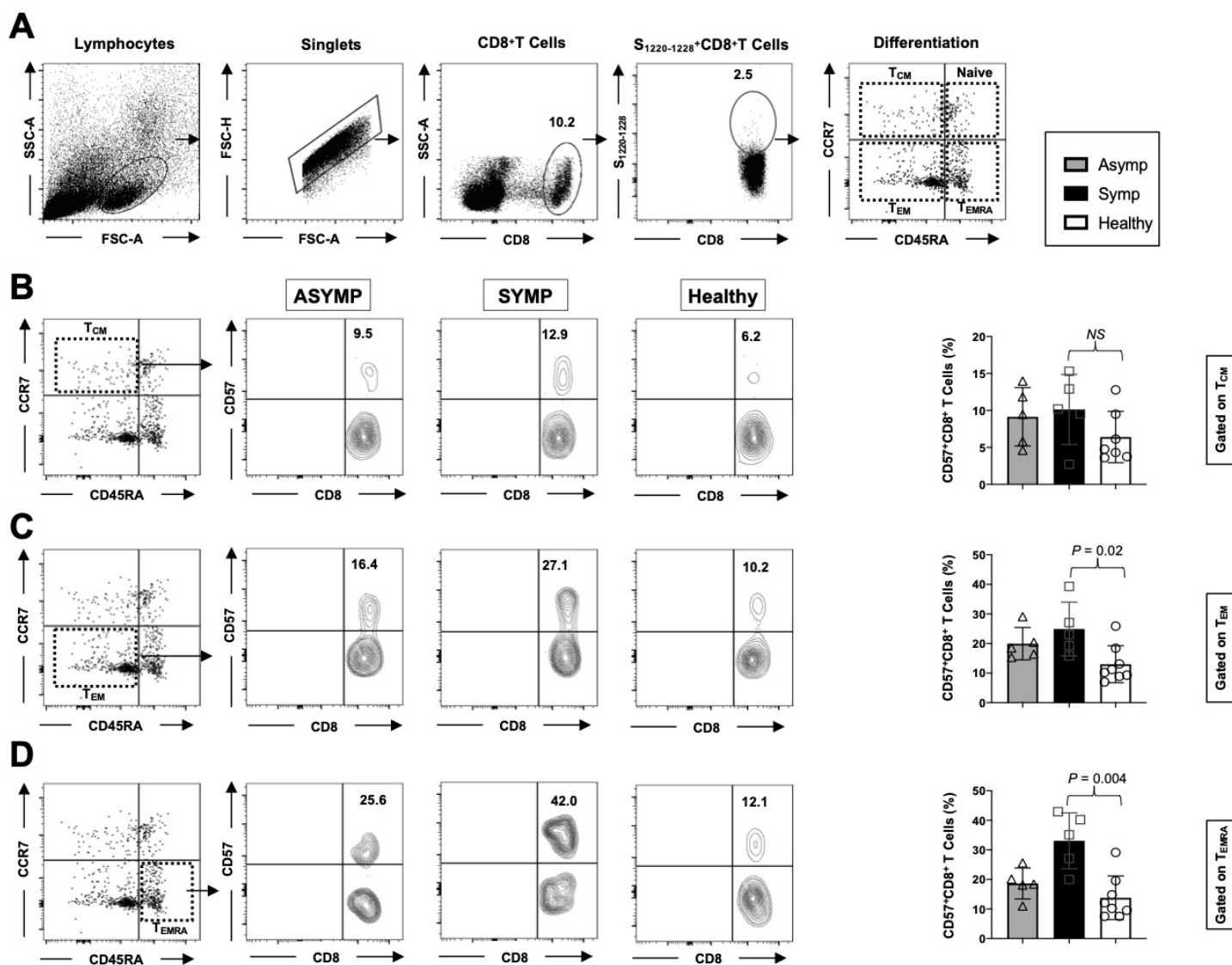


Fig. 6. Srivastava et al.

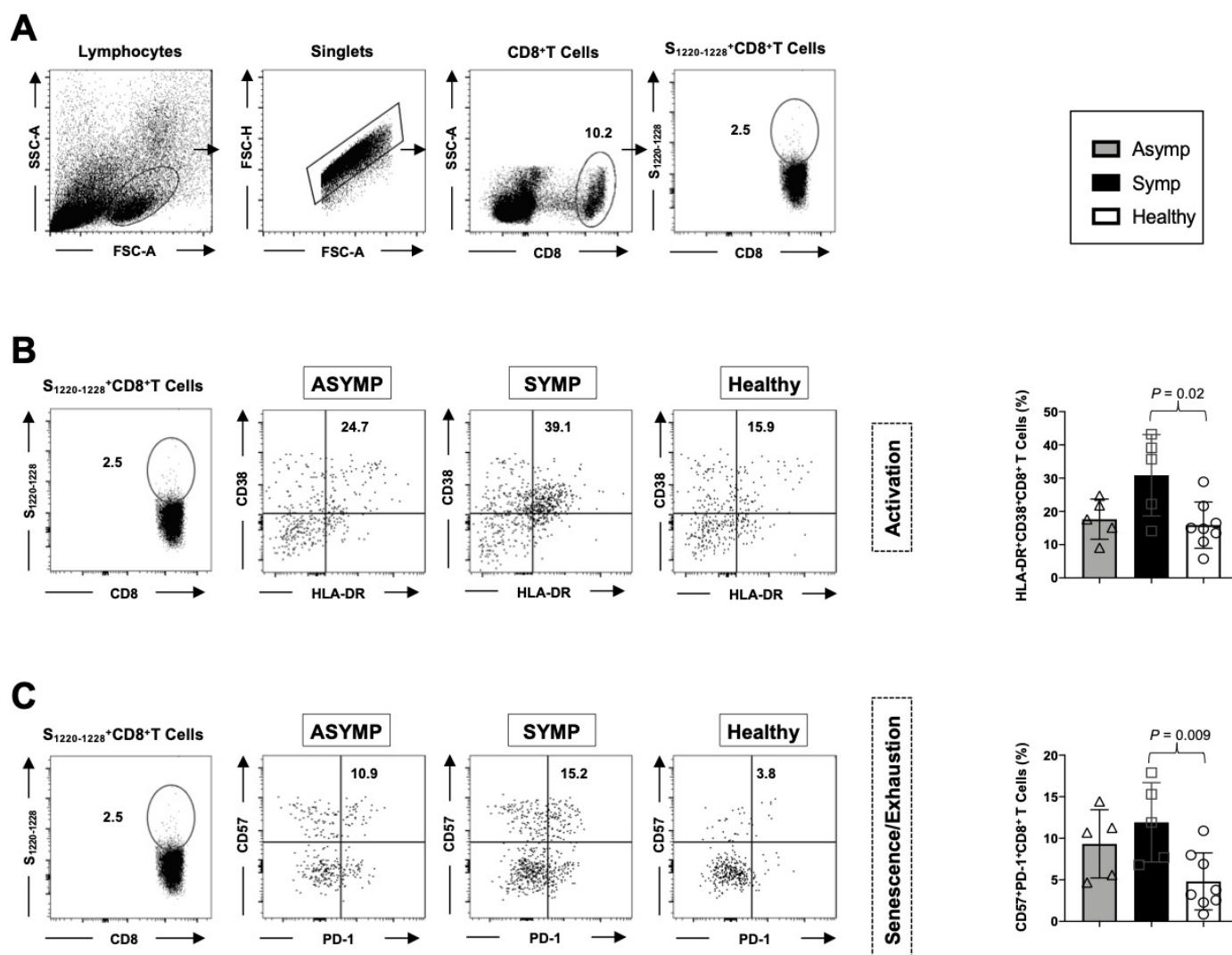
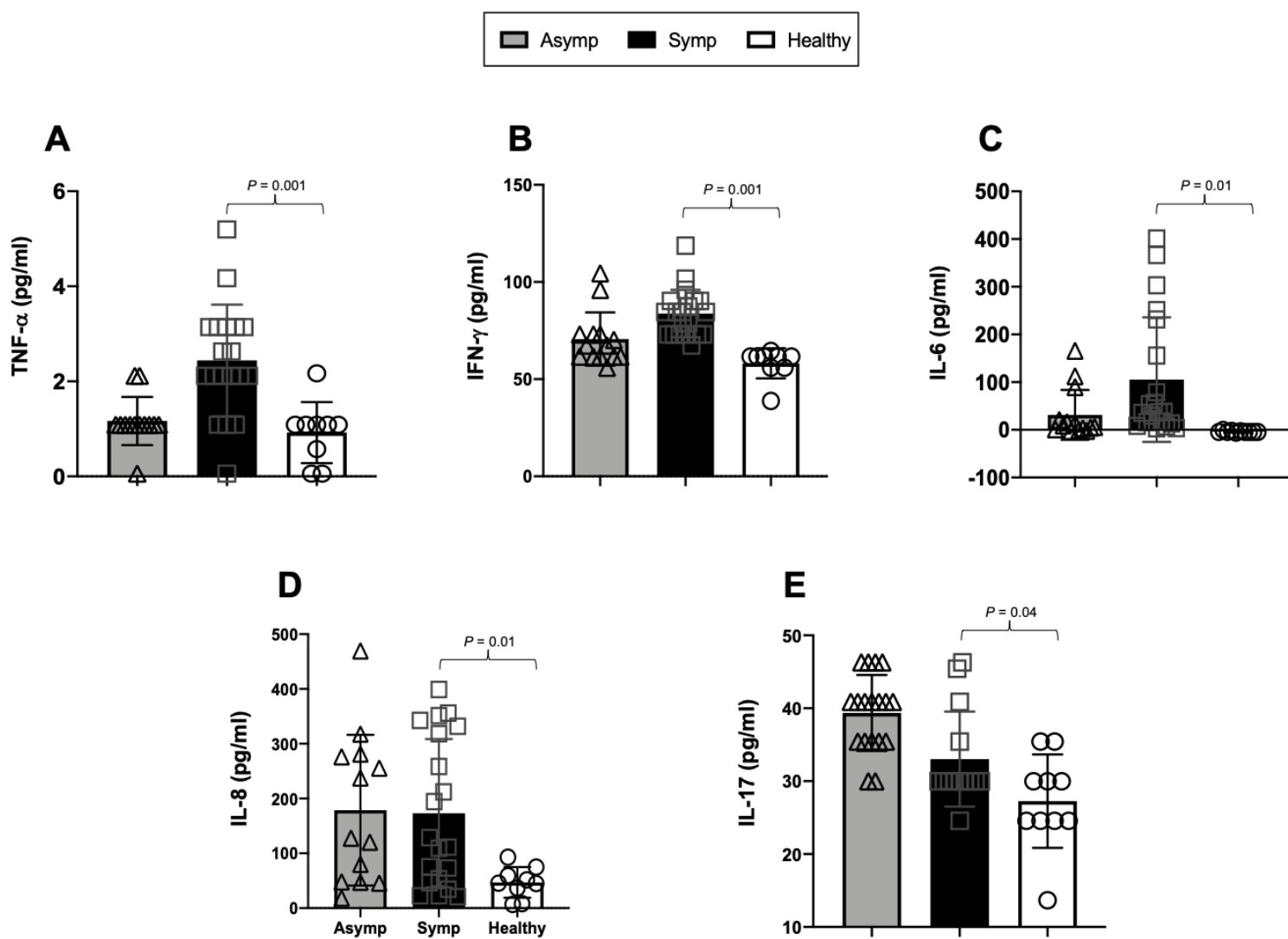


Fig. 7. Srivastava et al.



Cohorts of HLA-A2/HLA-DR positive, SARS-CoV-2 seropositive Symptomatic and Asymptomatic individuals enrolled in this study

Subject-level Characteristic	All Subjects (n = 20)
Gender [no. (%)]:	
Female	8 (40%)
Male	12 (60%)
Race [no. (%)]:	
Caucasian	6 (30%)
Non-Caucasian	14 (70%)
Age [median (range) yr.]:	39 (21-67 yr.)
SARS-CoV-2 status [no. (%)]:	
SARS-CoV-2-seropositive	20 (100%)
HLA [no. (%)]	
HLA-A2-positive	20 (100%)
HLA-DR-positive	20 (100%)
COVID-19 Disease Status [no. (%)]	
Asymptomatic (ASYMP)	10 (100%)
Symptomatic (SYMP)	10 (100%)